Available online at www.sciencedirect.com

ScienceDirect

Geochimica et Cosmochimica Acta 175 (2016) 239–251

Geochimica et Cosmochimica Acta

www.elsevier.com/locate/gca

A revised seawater sulfate oxygen isotope record for the last 4 Myr

Stefan Markovic [a,*], Adina Paytan [b], Hong Li [a], Ulrich G. Wortmann [a]

[a] Department of Earth Sciences, University of Toronto, 22 Russell St, Toronto, ON M5S3B1, Canada
[b] Institute of Marine Sciences, University of California Santa Cruz, Santa Cruz, CA 94064, USA

Received 17 February 2015; accepted in revised form 6 December 2015; Available online 14 December 2015

Abstract

Using a new method to purify barium sulfate from marine barite, we produce a highly resolved seawater sulfate oxygen isotope data set for the past 4 million years. We show that the overall magnitude of the $\delta^{18}O$ shift is smaller than previously thought (1–1.5‰ vs 6 ‰).

Expanding on previous work, we explore the effects of Quaternary sea level variations on the global sulfur cycle. Our modeling results confirm the earlier hypothesis that the increased duration and amplitude of sea level lowstands during the Quaternary favors direct sulfide oxidation over microbial disproportionation.

We show that oxygen isotope ratios of core top barite are up to 2.5‰ lower than the seawater sulfate $\delta^{18}O$ value. We hypothesize that this offset is caused by incorporation of sulfate from oxidized organic sulfur compounds during precipitation of barite. Our results provide another puzzle piece in the attempt to understand the origin of marine barite.

1. INTRODUCTION

It is generally assumed that marine barite records the oxygen isotope composition ($\delta^{18}O$) of seawater sulfate (Turchyn and Schrag, 2004, 2006, Griffith and Paytan, 2012), which enables us to trace the evolution of seawater sulfate $\delta^{18}O$ with time. However, using marine barite as recorder of the past seawater sulfate oxygen isotopic composition depends on obtaining pure barite samples free of other oxygen bearing mineral phases (e.g., iron oxides, silicates, rutile). Here we use an improved method of barite extraction and purification to produce a highly resolved marine $\delta^{18}O$-sulfate record over the past 4 Myr.

Previous sulfate $\delta^{18}O$ studies (Turchyn and Schrag, 2004, 2006) separated barite using gravity separation with lithium polytungstate (LST) heavy liquid. While elegant, this approach is unable to reliably separate barite from minerals with densities exceeding those of LST ~2.85 g/ml (e.g., various silicates, rutile) which may affect the $\delta^{18}O$ ratio of the respective sample.

To tackle the problem of contaminants we developed a new method to recover pure barium sulfate which involves: (1) sequential dissolution of carbonates, silicates, oxides and organic matter following Paytan et al. (1996); (2) an additional purification step which involves digestion of impure barite using sodium carbonate followed by precipitation of pure barium sulfate in an acidic medium, and subsequent heating treatment. This purification step will only dissolve barium sulfate, leaving any possible contaminants behind.

2. BACKGROUND

Continental shelves represent only 7–8% of the world ocean, but are responsible for ~80% of organic matter (OM) burial (e.g., Berner, 1982; Wollast, 1991; Hedges and Keil, 1995). Decomposition of this OM is mediated by a series of microbial respiration processes, which are controlled by the free energy yield of the respective redox

* Corresponding author. Tel.: +1 647 771 7750.
E-mail address: stefa.markovic@utoronto.ca (S. Markovic).

http://dx.doi.org/10.1016/j.gca.2015.12.005
0016-7037/

reaction (e.g., Froelich et al., 1979). The energetically most favorable redox reactions are aerobic respiration and denitrification, but both reactions are limited by the low concentration of the respective electron acceptors, oxygen and nitrate. Sulfate reduction, while energetically less favorable is promoted in the absence of oxygen and nitrate by high seawater sulfate concentrations (~28 mM in the present day ocean) and thus sulfate reducing bacteria respire ~50% of organic carbon and oxidize most of methane (e.g., Sørensen et al., 1979; Jørgensen, 1982; Canfield et al., 1993; Jørgensen and Kasten, 2006).

Microbial sulfate reduction (MSR) reduces sulfate to hydrogen sulfide, the majority of which is oxidized within the surface sediments (Jørgensen, 1982). Both MSR and sulfide oxidation, alter the oxygen isotope ratio of dissolved sulfate in the interstitial water (e.g., Fritz et al., 1989; Böttcher et al., 1998, 1999; Blake et al., 2006; Bottrell and Newton, 2006; Turchyn et al., 2006; Wortmann et al., 2007; Turchyn et al., 2010; Antler et al., 2013). The isotopically modified pore water sulfate will diffuse or get mixed into the overlying water column (sulfate reflux, Fig. 1), affecting the $\delta^{18}O$ of the ocean sulfate reservoir. The MSR and sulfate reflux are considerably larger than sulfate weathering inputs or burial fluxes (Fig. 1).

The MSR is a stepwise process with multiple reversible reactions and exchange fluxes between the cell interior of sulfate reducers and ambient water (Rees, 1973; Brunner and Bernasconi, 2005; Eckert et al., 2011). The sulfate transported into bacterial cells is first reduced to sulfite which may be further reduced to sulfide or oxidized and returned to the environment (e.g., Brunner and Bernasconi, 2005; Brunner et al., 2012). The oxygen isotope exchange between intracellular sulfite and water, and subsequent backflux of reoxidized sulfate, can produce O^{18} isotope enrichment in extracellular sulfate of up to 29‰ compared to seawater (~0‰, relative to Vienna Standard Oceanic Mean Water, hereafter VSMOW, e.g., Fritz et al., 1989; Van Stempvoort and Krouse, 1994; Wortmann et al., 2007; Turchyn et al., 2010; Antler et al., 2013; Wankel et al., 2014). However, the impact of these processes on the global seawater sulfate $\delta^{18}O$ value relative to other processes like sulfide oxidation or disproportionation reactions is not well constrained. Sulfate reducers continuously take up and consume isotopically altered porewater sulfate, which over time considerably reduces its backflux into seawater pool. Nevertheless, if we account the entire volume of sulfate that enters bacterial cells, the gross sulfate cycling could be considerably larger than the net reduction of sulfate to sulfide (Farquhar et al., 2008; Brunner et al., 2012; Wankel et al., 2014).

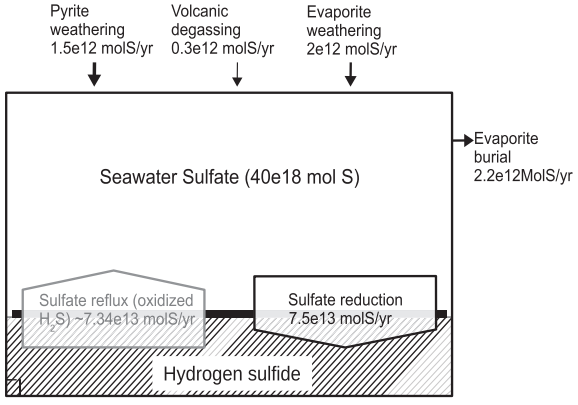

Fig. 1. Major fluxes controlling oxygen isotope ratio of seawater sulfate. Note: the arrow width is proportional to the flux. Flux data after Berner (1982), Kump (1989), Hansen and Wallmann (2003) and Jørgensen and Kasten (2006); see Supplementary file for full list. Note that sulfate reduction flux represents only the net MSR (i.e., the amount of sulfate reduced to sulfide), and excludes the cell internal cycling of sulfur intermediates which may exceed the volume of this flux twofold (Farquhar et al., 2008; Brunner et al., 2012; Wankel et al., 2014).

While it is difficult to quantify the relative importance of MSR vs different pathways of sulfide oxidation (e.g., Wortmann et al., 2007; Antler et al., 2013), we can use sulfate $\delta^{18}O$ signatures to broadly differentiate between sulfate modified by direct oxidation and sulfate that is affected by microbially mediated processes i.e., isotope exchange or fractionation during microbial sulfate reduction and disproportionation (Fig. 2). The $\delta^{18}O$ of sulfate produced during abiotic oxidation of sulfide is close to the oxygen isotope ratio of ambient seawater (0‰, relative to VSMOW, Taylor et al., 1984; Van Stempvoort and Krouse, 1994; see also Balci et al., 2007; Kohl and Bao, 2011; Balci et al., 2012). Similarly, microbial sulfide oxidation in the presence of an oxidant (e.g., O_2, nitrate, Fe(III) and Mn(IV)) imparts small, but variable O isotope offset (up to 8‰, Van Stempvoort and Krouse, 1994; Balci et al., 2012). In order to account for the overlapping $\delta^{18}O$ signatures of sulfate produced by abiotic and microbial direct oxidation, we will be using an umbrella term direct

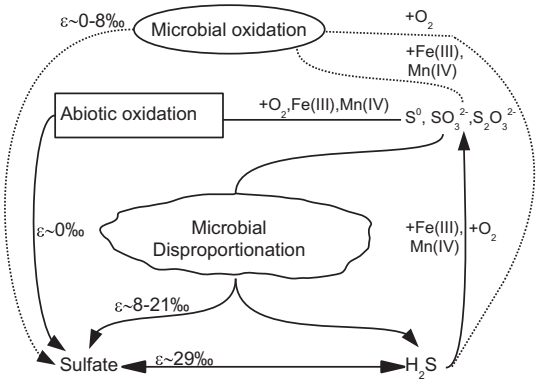

Fig. 2. Simplified schematic representation of the sulfur cycle. *Note:* The $\delta^{18}O$ value of sulfate produced during abiotic oxidation is close to that of ambient water (~0‰, Taylor et al., 1984; Van Stempvoort and Krouse, 1994) whereas microbial disproportionation imprints a distinct isotope offset (+8‰ to +21‰ relative to ambient water, Böttcher et al., 2001a,b, 2005). The microbial oxidation takes place in the presence of oxidant (O_2, Fe(III) and Mn(IV)) and imparts a variable isotope offset (up to 8‰, Van Stempvoort and Krouse, 1994; Balci et al., 2012). The reverse arrow between sulfate and sulfide represents oxygen isotope fractionation between sulfite and water during MSR (Fritz et al., 1989; Wortmann et al., 2007; Turchyn et al., 2010; Antler et al., 2013).

sulfide oxidation for both groups of processes. Microbial disproportionation in the presence of iron imparts sulfate oxygen isotope enrichments of 16–21‰ compared to ambient water (Böttcher et al., 2001a,b, 2005), while disproportionation in the presence of manganese offsets the $\delta^{18}O$ of sulfate by 8–12 ‰ (Böttcher et al., 2001a). On the other hand, kinetic fractionation and oxygen isotope exchange between the cell-internal sulfite and water during MSR offset the $\delta^{18}O$ of sulfate by up to 29‰ over the oxygen isotope composition of the water (e.g., Fritz et al., 1989; Wortmann et al., 2007; Turchyn et al., 2010; Antler et al., 2013).

Turchyn and Schrag (2004, 2006) suggested that the balance between direct sulfide oxidation and microbial sulfur disproportionation shows dependence on water depth, with the latter predominantly taking place in shallow environments and the former being more common in deep-sea areas. The rates of sulfur disproportionation are thought to be high in the shallow environments (Jørgensen, 1990; Thamdrup et al., 1993, 1994; Canfield and Thamdrup, 1994, 1996), promoted by high organic matter supply and rapid sulfur turnover. On the other hand, direct sulfide oxidation is important in sediments deposited in the upwelling areas (Ferdelman et al., 1997; Zopfi et al., 2008), submarine river fans (Aller et al., 1986; Canfield, 1989; Schulz et al., 1994; Aller et al., 2010), cold seep systems (Lichtschlag et al., 2010) and stratified marine environments (e.g., Black Sea, Burdige and Nealson, 1986; Oguz et al., 2001).

The $\delta^{18}O$ of seawater sulfate is controlled by the reflux of isotopically modified sulfate, input from continental weathering and volcanic emissions and output through evaporite precipitation (Fig. 1, for detailed discussion see Bottrell and Newton, 2006). Since the residence time of marine sulfate bound oxygen (~500 kyr, Jørgensen and Kasten, 2006) is short compared to rate of oxygen isotope exchange between dissolved seawater sulfate and ambient water (10^6–10^7 yrs, Llyod, 1967, 1968; Chiba and Sakai, 1985; Van Stempvoort and Krouse, 1994), dissolved sulfate preserves its original $\delta^{18}O$ signature. Furthermore, the marine residence time of sulfate bound oxygen exceeds the ocean mixing time (1600 yrs) by two orders of magnitude, so that the ocean can be considered a well mixed reservoir. The seawater sulfate $\delta^{18}O$ thus reflects the balance of its input and output fluxes at any given point in time.

In turn, the seawater sulfate $\delta^{18}O$ will be recorded by barite ($BaSO_4$) crystals forming in the water column (Turchyn and Schrag, 2004, 2006; Griffith and Paytan, 2012). Here we extract pure barite using our new two step method and produce a highly resolved and revised seawater sulfate $\delta^{18}O$ record. Furthermore, we complement our record with sulfur isotope measurements ($\delta^{34}S$) to get a better picture of global sulfur cycling in the past 4 Myr.

3. GEOLOGICAL SETTING

Once formed, barite is a very stable mineral. However, sediments where microbial sulfate reduction has depleted all dissolved sulfate, are prone to early diagenetic barite dissolution (e.g., Torres et al., 1996; Paytan and Griffith, 2007). Under these conditions barite can dissolve and reprecipitate as diagenetic barite elsewhere in the sediment column (Paytan et al., 2002). This process will change the barite sulfur and oxygen isotopic composition because the reprecipitated barite will acquire the pore fluid sulfate S- and O-isotope signal (Paytan et al., 2002; Griffith and Paytan, 2012), and it is thus important to select samples from locations where the concentration of sedimentary OM is low enough to prevent exhaustion of the dissolved sulfate pool.

We use core samples from leg 138 of the Ocean Drilling program (ODP), Site 849, which is located about 860 km west of the East Pacific Rise (0.1831°N, 110.5197°W) at a depth of 3850 m. At Site 849 organic matter concentrations are low and interstitial water sulfate concentrations remain high with depth (25–28 mM, Shipboard Scientific Party, 1992). We are thus certain that our samples are not affected by diagenetic barite dissolution and/or reprecipitation. This was confirmed with the SEM imaging analysis of crystal size and morphology which showed an absence of tabular, large (>10 μm) crystals suggestive of diagenetic barite (Paytan et al., 2002).

Sample ages are determined using high resolution (10–50 kyr) orbitally tuned age models by Shackleton et al. (1995).

The core top samples used in this study represent a range of sites and locations (see Supplementary data).

4. METHODS

We separated barite from sediment in two steps. The first step is sequential dissolution following Paytan et al. (1996) method. The second step involves barite digestion using sodium carbonate, reprecipitation in an acidic medium, and subsequent heating treatment. Each step in the method was tested using barite with a known $\delta^{18}O$ isotope composition (our $BaSO_4$ lab standard) to check for potential oxygen isotope exchange (see Supplementary file).

4.1. Sequential dissolution

Samples were treated with: (I) HCl to remove carbonates; (II) sodium hypochlorite to oxidize organic matter; (III) hydroxylamine hydrochloride to remove iron and manganese oxyhydroxides; (IV) concentrated HF-HNO_3 mixtures with ratios of 1:2, 1:1, and 2:1 to remove silicates; (V) aluminum chloride in 1 M HNO_3 to remove fluorides; (VI) heated at 750 °C in the furnace for 1 h to oxidize highly refractory organic matter. After each step (I–V), we centrifuged the samples, decanted the supernatant and washed the residue three times with ultrapure deionized water. We examined the purity of the extracted barite using X-ray diffraction spectra and used SEM imaging/EDS analysis to check for the potential presence of diagenetic barite and impurities (Paytan et al., 2002).

4.2. Purification

To avoid contamination with residual mineral phases like rutile, we introduced an additional purification step which involves: (1) barite digestion in sodium carbonate

solution (Breit et al., 1985; Von Allmen et al., 2010, with some modifications, see below); (2) subsequent reprecipitation of pure $BaSO_4$.

4.2.1. Digestion and reprecipitation

The sample residue obtained during the sequential dissolution step was weighed and placed in Axygen® 1.5 mL MaxyClear snaplock polypropylene microtubes. Next, we added 10 times the sample weight sodium carbonate (99.95%, Acros Organics) and 1 mL of miliQ water (resistivity > 18 MΩ). Microtubes were closed and placed in an oven, previously set at 85 °C and left to react for 24 h. The reaction between barium sulfate and sodium carbonate is a simple exchange of carbonate for sulfate, which produces barium carbonate precipitate while sulfate is released into solution:

$$BaSO_{4(s)} + Na_2CO_{3(aq)} \rightarrow BaCO_{3(s)} + Na_2SO_{4(aq)} \quad (1)$$

We separated the two phases using a centrifuge and decant the solution into larger BD Falcon™ 10 mL tubes. The supernatant liquid was acidified to pH 1 using trace metal grade hydrochloric acid and then 2–5 mL of 10% solution of $BaCl_2$ (99.9% Sigma–Aldrich) was added to precipitate pure $BaSO_4$:

$$Na_2SO_{4(aq)} + BaCl_2 \rightarrow BaSO_{4(s)} + 2NaCl_{(aq)} \quad (2)$$

The barium sulfate precipitate was left at room temperature overnight in the mother solution to "age". Next day samples were centrifuged and the liquid was decanted. Following this step, miliQ water (resistivity > 18 MΩ) was added to the tube, the remaining precipitate was shaken, centrifuged and decanted again. This "washing" step was repeated 5–7 times, to obtain precipitate free from $BaCl_2$ and HCl residues. To eliminate hydration water which is sorbed on, or trapped in the crystalline lattice (Walton and Walden, 1946a,b), the reprecipitated barium sulfate was heated at 700 °C for 1 h.

4.3. Mineral composition and chemistry of separated and purified barite

X-ray diffraction (XRD) was used to determine the mineral composition of bulk impure barium sulfate, reprecipitated synthetic barium sulfate and residuals after dissolution step.

Samples for XRD analysis were prepared by mixing a small amount of material (several mg) in ethyl-alcohol or acetone in order to make thick suspension which is than evenly smeared on zero reflection silica plate. XRD analysis was done on a Philips XRD system with a PW 1830 HT generator, a PW 1050 goniometer, PW 3710 control electronics, and X-Pert system software. The scanning speed was 2s per 1"; 2 theta ranges were 2–60°/70°.

Field emission scanning electron microscope system ZEISS SUPRA VP55 with INCA 350 Energy Dispersive X-ray detector (EDS) was used for micron scale imaging and microanalysis of reprecipitated barium sulfate and residuals following both sequential dissolution and purification step.

For XRD we estimate that under our setup detection limit for phases other than barite is between ~5 wt% for quartz (and other silicates) and 10 wt% for iron oxide and sodium carbonate phases. However, for SEM–EDS spot analysis detection limits for specific elements are minimum 0.1 wt%.

4.4. Isotope analysis

We analyzed the oxygen isotope ratios with a continuous flow isotope ratio monitoring mass spectrometry system using a Hekatech high temperature pyrolysis furnace coupled via a Finnigan Conflo III open split interface to a Finnigan MAT 253 mass spectrometer. Solid barite samples (~200 μg) were weighed into a silver capsule and introduced into pyrolysis furnace where $BaSO_4$ is converted to CO gas at 1400 °C under a helium atmosphere.

We also measured sulfur isotopic composition of those samples with enough remaining material. For sulfur isotope analysis solid barite samples (200 μg) were mixed in a tin cup with ~600 μg of V_2O_5 powder and introduced into Eurovector Elemental Analyzer (EA) where $BaSO_4$ is converted to SO_2 by combustion in a flush of oxygen.

Measurements were calibrated using international sulfate standards NBS 127 (+21.1‰, Vienna Canyon Diablo Troilite – VCDT; +8.6‰, VSMOW), IAEA SO5 (+0.49‰, VCDT; +12.13‰, VSMOW), IAEA SO6 (−34.05‰, VCDT; 11.35‰, VSMOW), USGS 32 (+25.4‰, VSMOW) (Coplen et al., 2001; Böhlke et al., 2003; Brand et al., 2009) and an in-house synthetic $BaSO_4$ (Sigma–Aldrich) standard (8.6‰, VCDT; 11.9 ± 0.2‰,VSMOW).

Repeated measurements of the in-house standard (typically >10 measurements per run) and international standards (3–4 measurements per standard per run) yield reproducibility of 0.15‰ (1 standard deviation – 1σ) for sulfur and 0.2‰ (1σ) for oxygen isotope measurements.

4.5. Statistical analysis

Uncertainties of the isotope data include errors in sample assigned ages and uncertainties in how well a single measurement represents the seawater sulfate S and O isotope value. Note that the latter uncertainty comprises not only the analytical precision (which can be quantified), but also sample origin, sample handling, and sample extraction. We therefore have to assume that each measurement carries an unknown error (or noise).

However, the seawater sulfate isotope value at any given time (t) depends to a certain degree on its isotope value at the time before. This coupling allows us to apply "local regression smoothing" (LOESS, Cleveland, 1979) to estimate the likely sulfate S and O isotope values.

We used the default LOESS module provided by the statistical software package R (R Development Core Team, 2013). The 95% confidence interval was calculated for each data point from the standard errors returned by the LOESS function and represents our best estimate of uncertainty associated with single isotope measurement at any point in time.

4.6. Sulfur cycle model

Our model is derived from Markovic et al. (2015) sulfur cycle model which is expanded to include the MSR and sulfate recycling (for the full model description see Supplementary file and Markovic et al., 2015 in addition to this section).

The model setup and boundary conditions are very similar to sulfur cycle isotope mass balance model by Turchyn and Schrag (2004, 2006). The model is built on the following assumptions: (a) The size of sulfate reservoir is not constant but increases as a result of pyrite and evaporate weathering during glacial shelf sediment exposure; (b) the rate of MSR and the balance between direct sulfide oxidation and microbial disproportionation varies depending on the extent of shelf area; (c) the expanded shelf area coincides with the high sulfate turnover through MSR and microbial disproportionation which increases seawater sulfate $\delta^{18}O$. In contrast, in times of reduced shelf abiotic sulfide oxidation dominates which decreases oxygen isotope composition of seawater sulfate. (d) The flux representing oxygen isotope fractionation during sulfate reduction is assumed to be equal to net sulfate reduction, i.e., for every sulfate molecule reduced to sulfide, the oxygen in one other sulfate is exchanged with water. This is well within the range of estimates for sulfate recycling during MSR based on compilation of batch culture and flow-through reactor experiments (Brunner et al., 2012), modeling of natural pore-water profiles (Antler et al., 2013) and previous models of global sulfur cycling (Turchyn and Schrag, 2004, 2006). (e) Since residual pore-water sulfate may not always attain the maximum O-isotope fractionation (Antler et al., 2013), the average oxygen isotope fractionation during MSR is assumed to be 14‰ compared to seawater (0‰ VSMOW), which is roughly halfway between seawater $\delta^{18}O$ and O isotope equilibrium of 29‰ (Fritz et al., 1989). This is in line with previous modeling studies which also employed similar values (7–14‰, Turchyn and Schrag, 2004, 2006).

The model first calculates the shelf area using sea level estimates by Miller et al. (2011) and cubic polynomial fit (from Bjerrum et al., 2006) of the global hypsometric curve ETOPO-5 (see Supplementary file). Next we take the fluxes which are affected by sea level change (sulfate reduction, sulfide reoxidation, pyrite and evaporite weathering and pyrite burial) and divide them in two boxes, the one of which represents background flux while the other varies in proportion to calculated shelf area.

The sulfate reduction flux is calculated as follows (3):

$$F^{*}_{MSR} = F_{MSR} * \left[1/2 + 1/2 * \frac{A_s - A_{min}}{A_{current} - A_{min}}\right] \quad (3)$$

where F^{*}_{MSR} is calculated sulfate reduction at any point in time F_{MSR} is the present day MSR estimate. A_s is the shelf area at each step. A_{min} and $A_{current}$ are minimum and present day extent of shelf area, respectively. We assume that out of the total MSR, half takes place in the shelf (up to 130 m depth) while the other half takes place in the deep water regions (abyssal and continental slope bellow 130 m of depth). These numbers are in good agreement with the present day spatial distribution of sulfate reduction in sediments at different water depth (Jørgensen, 1982; Jørgensen and Kasten, 2006; Thullner et al., 2009).

The estimates of the present day MSR rates vary considerably (Jørgensen and Kasten, 2006; Bowles et al., 2014). Initially we run the model using the estimate of $7.5 * 10^{13}$ mol S/yr, after Jørgensen and Kasten (2006). In the subsequent sensitivity tests, we run model experiments assuming present day MSR rates of $1 * 10^{13}$ mol S/yr and 10^{14} mol S/yr and using the same forcing.

The flux representing sulfate-oxygen fractionation during MSR is calculated as follows (4):

$$F_{exchange} = F^{*}_{MSR} * \left[1/2 + 1/2 * \frac{A_s - A_{min}}{A_{current} - A_{min}}\right] \quad (4)$$

$F_{exchange}$ represents oxygen isotope fractionation during MSR either by kinetic or equilibrium fractionation. Since sulfate fractionated during MSR may be mixed back to the seawater pool or eventually consumed by sulfate reducers, the size of this flux may be considerably smaller. Therefore, with respect to the oxygen isotope fractionation during MSR we tested two model scenarios. First, we assumed there was no mixing between sulfate fractionated during MSR and seawater sulfate. In the subsequent model runs, 50% of sulfate fractionated during MSR was mixed back to the seawater sulfate pool.

A fraction of MSR produced sulfide is buried as pyrite. The pyrite burial (F_{bp}) is calculated as follows (5):

$$F_{bp} = F_{bp\text{-}abyssal} + F_{bp\text{-}shelf} * \frac{A_s - A_{min}}{A_{max} - A_{min}} \quad (5)$$

where $F_{bp\text{-}abyssal}$ corresponds to the minimum pyrite burial which takes place in slope and abyssal environments at minimum shelf extent in this case $0.6 * 10^{12}$ mol S/yr, $F_{bp\text{-}shelf}$ is the portion of pyrite that is buried on the shelf at the maximum shelf extent (A_{max}) assumed to be $1.4*10^{12}$ mol S/yr; A_{min} is the minimum shelf extent and A_s is the shelf area at each step. These numbers are based on present day estimates of sulfate reduction rates and pyrite burial in sediments at different water depth (Jørgensen, 1982; D'Hondt et al., 2002; Jørgensen and Kasten, 2006; Thullner et al., 2009).

Sulfate reflux (F_{reox}) is calculated from known F^{*}_{MSR} and pyrite burial at each point in time (6):

$$F_{reox} = F^{*}_{MSR} - F_{bp} \quad (6)$$

The $\delta^{18}O$ ratio of sulfate from oxidized sulfide ($\delta^{18}O_{Freox}$) depends on the pathway of reoxidation (Fig. 2) and the oxygen isotope composition of seawater ($\delta^{18}O_{sw}$). At present day $\delta^{18}O_{sw}$ is on average 0‰ (VSMOW). However, it has varied in the past across glacial-interglacial cycles. For example, the waxing of ice sheets in glacial stages increases $\delta^{18}O$ of ocean water (e.g., Shackleton, 1967, 1987). Pore water studies constrain the amplitude of seawater oxygen isotope variations due to the growth of ice sheets but only for the most recent glacials. For the last glacial maximum (LGM) the estimated change is $+ 1.0 \pm 0.1$‰ (Schrag et al., 1996, 2002; Adkins et al., 2002). Since Miller et al. (2011) sea level record is based on benthic foraminifera $\delta^{18}O$ (Lisiecki and Raymo,

2005), it also reflects fluctuations in the mass of polar ice caps. Therefore, sea level change is proportional to the seawater $\delta^{18}O$ value if oxygen isotope composition of the polar ice did not change between last glacial maximum and previous Quaternary glaciations. Assuming that O isotope composition of polar ice remained the same, we extrapolated the LGM estimates into the rest of Quaternary, in order to assess what would be the effect of fluctuating seawater $\delta^{18}O$ on sulfur cycle. The $\delta^{18}O_{Freox}$ is calculated using the following (7):

$$\delta^{18}O_{Freox} = \delta^{18}O_{sw} + \delta^{18}O_{interglacial} - \left[\delta^{18}O_{interglacial} - \delta^{18}O_{glacial}\right] * \frac{A_{max} - A_s}{A_{max} - A_{min}} \quad (7)$$

where $\delta^{18}O_{Freox}$ is $\delta^{18}O$ ratio of sulfate from oxidized sulfide, $\delta^{18}O_{sw}$ is estimated seawater $\delta^{18}O$ ratio, $\delta^{18}O_{interglacial}$ is maximum $\delta^{18}O_{Freox}$ corresponding to maximum shelf flooding, $\delta^{18}O_{glacial}$ is $\delta^{18}O_{Freox}$ during Pleistocene sea level minimum. The assumed values for $\delta^{18}O_{interglacial}$ and $\delta^{18}O_{glacial}$ are different for two model scenarios. In model scenario I, $\delta^{18}O_{interglacial}$ and $\delta^{18}O_{glacial}$ are assumed to be between 8.4‰ and 3‰, while in model scenario II, these are 4.3‰ and 0.8‰ respectively.

Thus calculated $\delta^{18}O_{Freox}$ represents composition of the sulfate reflux from oxidized sulfide (see Fig. 1). The $\delta^{18}O_{Freox}$ reflects the relative balance between direct sulfide oxidation and microbial disproportionation. The direct sulfide oxidation produces sulfate with $\delta^{18}O$ similar to that of ambient water (Taylor et al., 1984; Van Stempvoort and Krouse, 1994; Balci et al., 2007; Balci et al., 2012) which we assume to be on average 0‰ VSMOW (present day seawater $\delta^{18}O$). The case for $\delta^{18}O$ of sulfate produced during disproportionation is however more complicated, as the range of measured oxygen isotope signatures is very wide (8–21‰ VSMOW, Fig. 2). Here we assume that on average $\delta^{18}O$ of sulfate produced by disproportionation is 15‰ VSMOW, which allows us to estimate its relative contribution across glacial–interglacial cycles. Note that selection of the average sulfate $\delta^{18}O$ for microbial disproportionation has minor impact on model results/conclusions. The model $\delta^{18}O$ output and its fit with the data would not change if we selected some other value, e.g., 16‰ for microbial disproportionation. In this case, calculated relative contribution of this process across glacial–interglacial cycles would be about −2% lower.

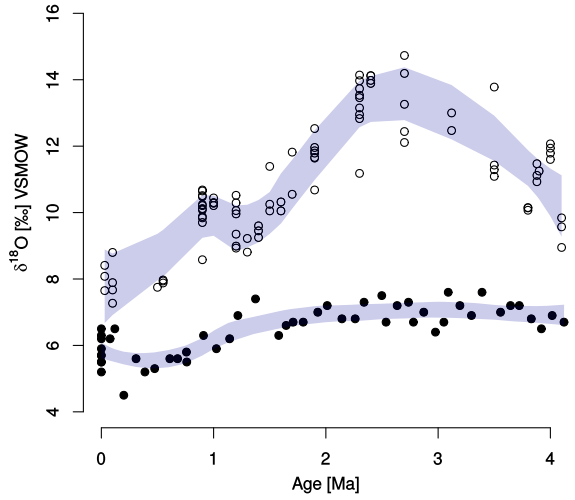

Fig. 3. Barite $\delta^{18}O$ results. The black full circles denote the average measured barite $\delta^{18}O$ for each sample (this study – see Supplementary file for tabulated results) and open circles are individual barite $\delta^{18}O$ measurements from Turchyn and Schrag (2004), the shaded area represent the 95% confidence intervals of a LOESS approximation of the "true" $\delta^{18}O$ value (see Section 4) for both records. Note that the difference between two date sets reflects in part an assigned $\delta^{18}O$ value for international NBS 127 standard. In this study we use recently recalibrated value of 8.6‰ VSMOW (Brand et al., 2009) while Turchyn and Schrag (2004) used earlier assigned value of 9.3‰ VSMOW, which shifted their results towards more positive values by 0.7‰.

5. RESULTS

The marine barite $\delta^{18}O$ varies between 4.4‰ and 7.6‰ (VSMOW) with an average value of 6.5‰ (Fig. 3). Between 4.1 Ma and 1.2 Ma, $\delta^{18}O$ fluctuate around 7‰ with a standard deviation (1σ) of 0.4‰ (twice the analytical uncertainty of 0.2‰). However, from 1.2 Ma we observe a steady decline from 7‰ to ~6‰ in the most recent sediments. The $\delta^{18}O$ of the core top samples falls between 5.5‰ and 6.5‰, with a mean of 6‰ and 1σ of 0.4‰.

The $\delta^{34}S$ data shows stable values that fluctuate around ~22‰ (VCDT) with a standard deviation (1σ) of 0.3‰ before 2 Ma. Between 2 Ma and 0.7 Ma we observe a steady decline from ~22‰ (VCDT) to 21‰ (VCDT) (Fig. 4). In the past 0.7 Ma $\delta^{34}S$ values are relatively stable around 21‰ (VCDT) (Fig. 4).

6. DISCUSSION

The oxygen isotope values of our barite samples are up to 7‰ lighter than the previously published record of

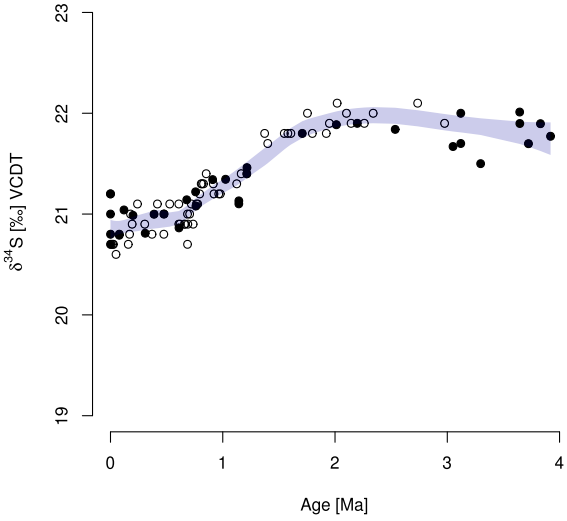

Fig. 4. Barite $\delta^{34}S$ results. Full black circles denote measurements of samples from this study (see Supplementary file for tabulated results), open circles denote data from Markovic et al. (2014), the shaded area the 95% confidence interval of a LOESS approximation of the "true" $\delta^{34}S$ (see Section 4).

Turchyn and Schrag (2004) (Fig. 3). There are two possibilities to explain this large offset: (1) Our results are affected by sulfate produced through oxidation of pyrite during sequential dissolution step, which would lead to anomalously low oxygen isotope ratios (DeBond et al., 2012) or (2) contamination of barite with other minerals (e.g., silicates, rutile), may be affecting oxygen isotope measurements in Turchyn and Schrag (2004) study.

While we selected samples from cores with low organic matter and stable pore water sulfate content (25–28 mM, Shipboard Scientific Party, 1992), which are unlikely to contain pyrite, based on sample selection alone we cannot completely exclude pyrite oxidation during extraction process. However, the pyrite content would vary from sample to sample which should lead to a different degree of pyrite contamination and result in a large spread of the $\delta^{18}O$ and $\delta^{34}S$ values (DeBond et al., 2012). Since our data clusters fairly well, we assume that pyrite oxidation has no major effect on our $\delta^{18}O$ measurements.

The main difference between our study and that of Turchyn and Schrag (2004) is the separation method used to extract barite. Heavy liquid separation method employed by Turchyn and Schrag (2004), does not discriminate between barite and minerals with densities exceeding optimal density of lithium polytungstate (2.85 g/ml), e.g., many silicates, rutile, and iron oxides. The oxygen isotopic ratios observed in these minerals can reach values up to 30‰ (VSMOW) (Hoefs, 2009), and any contamination would affect the $\delta^{18}O$ of the sample.

We adjusted our extraction procedures to address these problems, i.e., in order to extract pure barium sulfate we dissolved all barite to separate it from mineral phases like silicates, oxides or rutile which do not dissolve with Na_2CO_3. We demonstrate that barium sulfate is separated quantitatively from these contaminants (see Supplementary file). Additionally, to ensure that our sample extraction does not affect $\delta^{18}O$ composition of barite, each step in the method is tested using barium sulfate with known $\delta^{18}O$ (see Section 4 and Supplementary file for details). Therefore, we think that our data set is more likely to represent the uncontaminated marine barite $\delta^{18}O$ composition.

6.1. Causes of observed seawater sulfate $\delta^{18}O$ change

If we accept the premise that our data is a "true" recorder of the marine seawater sulfate $\delta^{18}O$ signal, the observed variations imply considerable changes in the oxygen isotopic composition and/or flux of sulfate into the ocean. Climatic variations during the Quaternary likely affected the weathering fluxes of sulfate/sulfide into the ocean (Markovic et al., 2015). However, these fluxes are small compared to the ocean sulfate reservoir and are unlikely to have large impact on the sulfate $\delta^{18}O$ signal on sub-million year timescales (see Fig. 1). On the other hand, changes of the balance between direct sulfate oxidation and disproportionation processes may have a significant impact on seawater sulfate $\delta^{18}O$. This balance is thought to be susceptible to variations of the submerged shelf area, which in turn is greatly affected by glacial-interglacial sea level variations.

During interglacials, high sea levels resulted in expanded shelf areas that are characterized by high OM burial rates and intense microbial carbon turnover through MSR (Jørgensen, 1982; Berner, 1982). Bioturbation and the abundant iron and manganese oxyhydroxides supplied by weathering on continents, promote oxidation of hydrogen sulfide to intermediate sulfur compounds, which favors sulfur cycling through microbially mediated disproportionation (Thamdrup et al., 1993, 1994; Canfield and Thamdrup, 1994; Canfield and Thamdrup, 1996). High rates of sulfur cycling through disproportionation processes impart distinct sulfate $\delta^{18}O$ enrichment.

During sea level lowstands, however, shelf areas supporting the above processes are much smaller and replaced by low-lying coastal plains transected by rivers. This reduces global MSR rates, the total production of sulfide, and its subsequent oxidation to sulfate. The narrowing of continental shelf pushes upwelling areas further offshore while riverine sediment load is funneled through submarine canyons to continental slope and abyssal plain. Consequently direct sulfide oxidation, which is common in modern deep sea fans (Aller et al., 1986; Canfield, 1989; Schulz et al., 1994; Aller et al., 2010) and upwelling areas (Ferdelman et al., 1997; Zopfi et al., 2008) becomes more important. Furthermore, continental shelf areas are being eroded and pyrite and organic S contained in these shelf sediments are being oxidized which produces sulfate with $\delta^{18}O$ close to that of the ambient water, (e.g., Taylor et al., 1984; Balci et al., 2007) thus lowering seawater sulfate $\delta^{18}O$ as well. Note that the conversion of pyrite to sulfate will affect the seawater sulfate concentration as well as its sulfur isotope composition. The latter effect is indeed visible in the ~1‰ negative shift of seawater sulfate $\delta^{34}S$ in the past 1.5 Myr (Fig. 4; see also Markovic et al., 2015 for detailed discussion).

6.2. Model results

We explore the impact of sea level variations on the global sulfate fluxes using a sulfur cycle model from Markovic et al. (2015) which was modified in order to simultaneously calculate changes in $\delta^{34}S$ and $\delta^{18}O$ of seawater sulfate.

The model first calculates the ocean covered shelf area (Fig. 5) using Miller et al. (2011) sea level estimates. Subsequently, we use the shelf area to calculate: sulfate input and output fluxes, MSR and sulfate reflux from oxidized sulfide, the oxygen isotope ratio of sulfate reflux as well as the relative proportion of microbial disproportionation and direct sulfide oxidation (Fig. 6., see Section 4 and Supplementary file for a detailed model description).

Model outputs (Fig. 7) capture the concurrent decline of $\delta^{18}O$ and $\delta^{34}S$ values in the past 2 Myr, supporting the notion that the intensification of the Quaternary glaciation and its effect on the areal extent of shelf had a considerable impact on the balance between different pathways of sulfur cycling (direct sulfide oxidation vs. microbial disproportionation, Turchyn and Schrag, 2004, 2006 and sulfur erosion/burial fluxes Markovic et al., 2015).

The shape of $\delta^{18}O$ output is sensitive to different estimates of the modern MSR used to initialize model

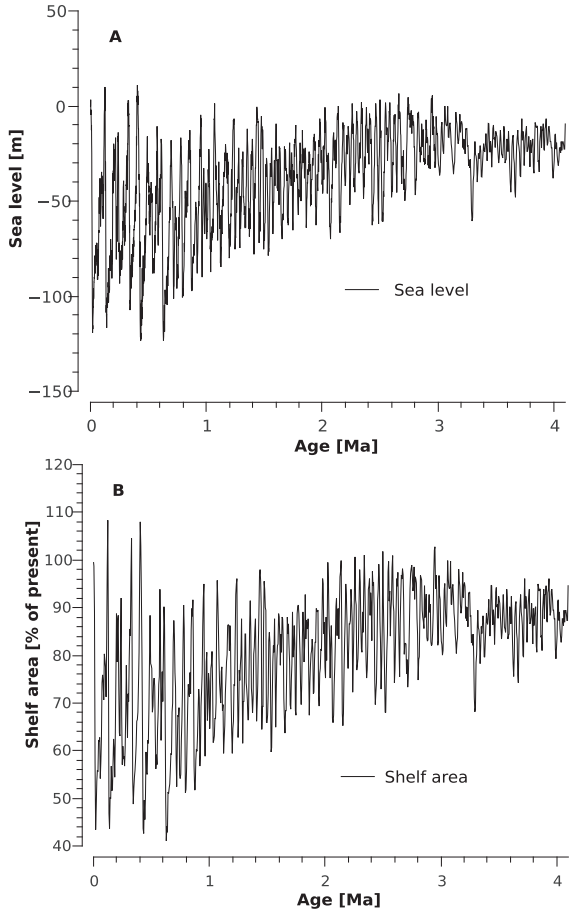

Fig. 5. Sea level and shelf area estimate. (A) Sea level estimate (Miller et al., 2011). (B) Calculated shelf area using polynomial fit (Bjerrum et al., 2006) of ETOPO-5 global mean hypsometric curve.

(Fig. 7A and B). The effect of periodic forcing on the isotopic composition of oxygen in sulfate depends on its residence time and periodicity of forcing (Richter and Turekian, 1993). Since for each model scenario we do not change the model forcing, the order of magnitude change in the residence time of sulfate oxygen (400 yr to 4 Myr, for selection of MSR of 10^{14} mol S/yr and 10^{13} mol S/yr, respectively) is reflected in different model response (Fig. 7A and B).

In the sensitivity runs assuming global MSR at 10^{14} - mol S/yr the model response to sea level forcing is quicker and amplified. However, the output is similar to the main model run and falls within the 95% confidence interval of $\delta^{18}O$ data except in the past 0.5 Myr, when it overshoots the $\delta^{18}O$ signal.

The model run assuming MSR rates of 10^{13} mol S/yr (comparable to $1.13 * 10^{13}$ mol S/yr estimate by Bowles et al., 2014) falls within 95% confidence interval of $\delta^{18}O$ data before 1.5 Myr and undershoots the $\delta^{18}O$ data after 1.5 Myr (Fig. 7A). Since MSR and sulfate reflux calculated here are only 2–5 larger than sulfate input from pyrite weathering (Fig. 6A and C), this model experiment represents primarily sulfate $\delta^{18}O$ isotope variations resulting from increased pyrite weathering on the shelf. Although increased pyrite weathering affected seawater sulfate $\delta^{34}S$ in Quaternary (Fig. 7C; see also Markovic et al., 2015), the impact on seawater sulfate $\delta^{18}O$ is much smaller, because the isotope offset between sulfate produced by pyrite oxidation and seawater sulfate is only −8.6‰ (~0‰ VSMOW vs. 8.6‰ VSMOW, Van Stempvoort and Krouse, 1994; Johnston et al., 2014), significantly less than sulfur isotope offset of ~−40‰. Therefore, if we assume the low estimate for MSR rates, the increased pyrite weathering produces only a modest change of ~−0.5‰ which is not enough to reproduce the magnitude or shape of our seawater sulfate $\delta^{18}O$ signal (Fig. 7A). If we were to reproduce the full $\delta^{18}O$ shift the oxygen isotopic composition of sulfate reflux during glacials would have to be 0‰ VSMOW, i.e., it would be completely dominated by abiotic sulfide oxidation. Since this is unlikely, Bowles et al. (2014) MSR estimate may be too low or unrepresentative for Quaternary.

In model scenario II, the oxygen isotope exchange during MSR represents an amplifier, creating a more dynamic system with higher sulfate-oxygen turnover. In order to produce the negative $\delta^{18}O$ shift in the past 2 Myr we need a large source of sulfate with low $\delta^{18}O$ values to counterbalance the impact of isotopically enriched sulfate-oxygen produced during MSR. There are only two possible sources that could be invoked—pyrite weathering and direct oxidation of reduced sulfur species coupled with iron, manganese or nitrate reduction. Since the former process would also introduce significant change of sulfate $\delta^{34}S$ which are not supported by barite sulfur isotope data, the latter process is the most likely candidate. Thus, in model scenario II, the direct oxidation during glaciations dominates the overall sulfate reflux; the $\delta^{18}O$ of sulfate produced during oxidative sulfur cycling drops to ~0‰ during the most severe glaciations (see Fig. 6 for forcing fluxes).

Note that in model scenario II only 50% of sulfate fractionated during MSR is mixed into seawater sulfate pool. Larger flux would require unrealistically big source of sulfate of O^{18} depleted sulfate to counterbalance it. For instance, if the entire volume of sulfate fractionated during MSR returns to the seawater pool, the model $\delta^{18}O$ output would increase monotonically even with the complete dominance of direct oxidation (i.e., assuming that $\delta^{18}O$ of sulfate reflux from oxidized sulfide is 0‰ throughout the model run). Since the oxygen isotope value of sulfate reflux is unlikely to be lower than seawater $\delta^{18}O$, we suggests that most of sulfate fractionated during MSR is eventually consumed by sulfate reducers. The small positive shift in our $\delta^{18}O$ data set for the past 200 kyr is not captured by model results. This shift may represent changes in shelf bathymetry. Late Pleistocene interglacial shelf is likely much deeper compared to earlier periods, reflecting significant sediment offloading during the first 100 kyr sealevel lowstands (Hay and Southam, 1977; Markovic et al., 2015). The MSR rates in deeper water settings are lower (e.g., D'Hondt et al., 2002, Bowles et al., 2014; see also compilation of rates in Jørgensen and Kasten, 2006). Since lower sulfate reduction rates result in higher oxygen isotope fractionation during MSR (Böttcher et al., 1998, 1999; Antler et al., 2013) it is possible that this deepening of the shelf may have shifted seawater sulfate $\delta^{18}O$ towards higher values, which is not

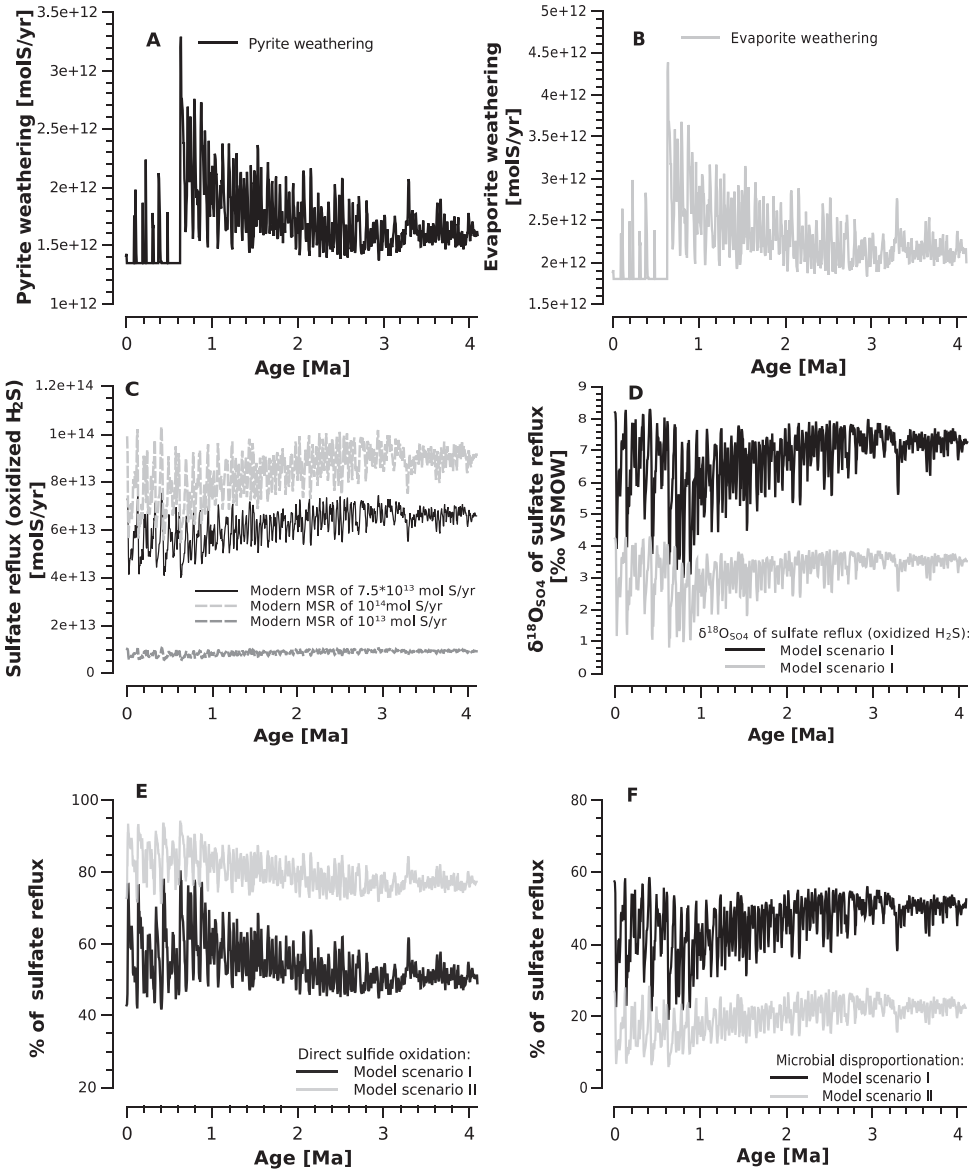

Fig. 6. Model forcing – the impact of sea level variation on fluxes controlling oxygen isotopic composition of seawater sulfate. (A) Pyrite weathering. (B) Evaporite weathering. (C) Reflux of isotopically modified sulfate (calculated as a difference between MSR and pyrite burial). (D) Oxygen isotopic composition of isotopically modified sulfate. (E) Direct sulfide oxidation expressed as percentage of the total isotopically modified sulfate reflux. (F) Microbial disproportionation as percentage of the total isotopically modified sulfate reflux.

captured, because our model does not account for changes in shelf bathymetry.

6.3. The source of sulfate for barite precipitation

The barite core top $\delta^{18}O$ values diverge from modern seawater sulfate oxygen isotope signature by 2–2.5‰ (~8.6‰, VSMOW, Johnston et al., 2014 for seawater sulfate compared to 5.5–6.5‰ VSMOW in our dataset). Similar offset (1.5–2‰ see Fig. 3) was previously noted by Turchyn and Schrag (2004, 2006). They proposed that oxygen isotopes are kinetically fractionated during barite precipitation. However, kinetic isotope fractionation in other sulfate minerals (evaporitic gypsum or anhydrite) causes a positive oxygen isotope offset in both sulfur and oxygen isotope ratios (e.g., Lloyd, 1968; Holser et al., 1979), which is also expected in the case of barite. Since this is not the case and only $\delta^{18}O$ isotope signatures of barite are different from contemporaneous seawater sulfate, we suggest that alternative process—the oxidation of organic S compounds during barite precipitation in microenvironments of sinking organic matter is responsible.

Barite is thought to be formed in microenvironments which are supersaturated with respect to barium sulfate (e.g., Dehairs et al., 1980; Bishop, 1988; Ganeshram at al., 2003; Jacquet et al., 2007), while the rest of the water column is under-saturated (Monnin et al., 1999; Rushdi et al., 2000). These microenvironments are enriched in

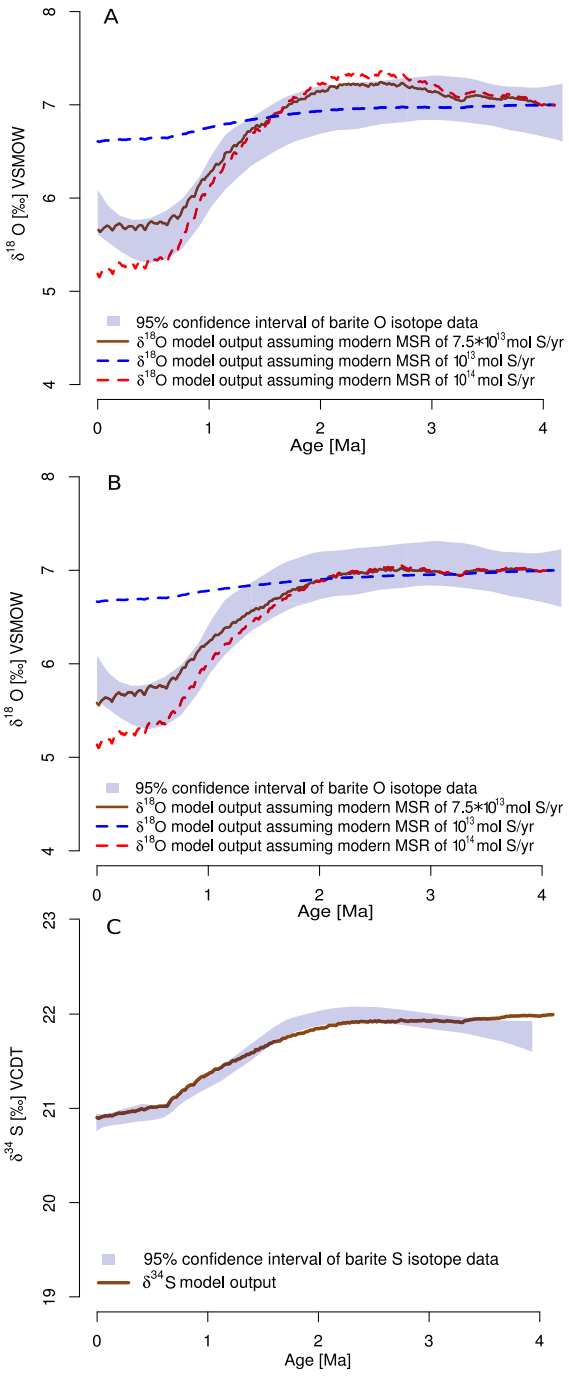

Fig. 7. Model output: (A) model scenario I (sulfate $\delta^{18}O$ output); (B) model scenario II (sulfate $\delta^{18}O$ output); the brown solid lines in A and B represent model assuming Jørgensen and Kasten (2006) modern MSR estimate of $7.5 * 10^{13}$ mol S/yr. The red and blue dashed lines represent model output assuming modern MSR of 10^{14} mol S/yr and $1 * 10^{13}$ mol S/yr respectively. (C) Seawater sulfate $\delta^{34}S$. Note that this model output is the same for all model runs. The brown solid line represents model $\delta^{34}S$ output. The shaded areas represent 95% confidence interval of a LOESS approximation of the "true" $\delta^{18}O$ and $\delta^{34}S$. (For interpretation of the references to colour in this figure legend, the reader is referred to the web version of this article.)

sulfate, from decaying organic matter (Chow and Goldberg, 1960; Bishop, 1988). Since incorporation of sulfate in organic matter (assimilatory sulfate reduction) produces very small S isotope fractionation (1–3‰, Canfield, 2001; Amrani, 2014), sulfate originating from organic S compounds in microenvironments of barite precipitation should have $\delta^{34}S$ value close to seawater sulfate (~21‰, VCDT). On the other hand, oxygen from seawater can be incorporated in product sulfate during oxidation of organic S compounds. Hence, barite $\delta^{34}S$ values are close to seawater sulfate (~21‰, see Fig. 4), while the O isotope values are shifted towards seawater oxygen isotope composition (0‰ VSMOW, Fig. 3).

This interpretation implies that the marine barite $\delta^{18}O$ signature represents oxygen isotope composition from two sources, with end members being seawater (0‰ VSMOW) and seawater sulfate (8.6‰ VSMOW). We can then calculate contribution of each end member using:

$$\delta^{18}O_{\text{core top}} = \delta^{18}O_{SO4} * A_{\text{SW-SO4}} + \delta^{18}O_{\text{reox-S}} * B_{\text{reox-S}} \quad (8)$$

where $A_{\text{SW-SO4}}$ and $B_{\text{reox-S}}$ are the fractions of O atoms coming from seawater sulfate and seawater respectively. Solving this equation gives 0.70 and 0.30 for oxygen for $A_{\text{SW-SO4}}$ and $B_{\text{reox-s,}}$ respectively. In other words, the relative contribution of sulfate coming from oxidized organic sulfur could be 30%. However, we don't know the isotopic composition of oxidized organic S which may be close to seawater $\delta^{18}O$ or higher depending on the pathway of sulfur oxidation. Therefore, this estimate could be the minimum contribution of oxidized organic sulfur.

7. CONCLUSION

It is difficult to separate marine barite from other mineral phases, e.g., silicates, iron or manganese oxides or rutile. These impurities represent a serious problem for oxygen isotope measurements, since they carry $\delta^{18}O$ signatures which are unrelated to that of barite. Using an improved method to recover pure barium sulfate we produced a new marine barite $\delta^{18}O$ record for the past 4 Ma. Our data suggests a 1–1.5‰ drop in the marine sulfate $\delta^{18}O$ in the past 2 Ma which is significantly less than previously thought (~−6‰ in Turchyn and Schrag, 2004).

In line with previous studies (Turchyn and Schrag, 2004, 2006) we show that the Quaternary glaciations and concomitant reduction in shelf area are likely to have a considerable effect on microbial sulfur cycling. Modeling results suggest that glacial periods saw 50–100% decrease in the microbial disproportionation during the most severe Quaternary glaciations.

We find that core top barite $\delta^{18}O$ values are 2–2.5‰ lower than modern seawater sulfate oxygen isotope signature and hypothesize that barite incorporates sulfate from two sources during precipitation. More work is needed to elucidate the origin and the underlying factors that control this offset. For instance, it is unclear if this offset changes depending on local conditions e.g., composition of organic matter in marine snow, size of sinking organic particles or presence of specific sulfur oxidizing bacteria.

ACKNOWLEDGMENTS

For helpful discussions and comments on early draft of this paper we thank Alexandra V. Turchyn, Yongbo Peng and Boswell Wing. Also we would like to acknowledge editorial input by James Farquhar (Associate Editor) and helpful reviews by Benjamin Brunner and 2 anonymous reviewers. SM wishes to acknowledge Zhongwu Ma for help with barite separation and for providing samples. This project was supported by a NSERC discovery grant to UGW and Keevil/Finley President's Fellowship in Geology to SM.

APPENDIX A. SUPPLEMENTARY DATA

Supplementary data associated with this article can be found, in the online version, at http://dx.doi.org/10.1016/j.gca.2015.12.005.

REFERENCES

Aller R. C., Mackin J. E. and Cox R. T. (1986) Diagenesis of Fe and S in Amazon inner shelf muds: apparent dominance of Fe reduction and implications for the genesis of ironstones. *Cont. Shelf Res.* **6**, 263–289.

Aller R. C., Madrid V., Chistoserdov A., Aller J. Y. and Heilbrun C. (2010) Unsteady diagenetic processes and sulfur biogeochemistry in tropical deltaic muds: implications for oceanic isotope cycles and the sedimentary record. *Geochim. Cosmochim. Acta* **74**, 4671–4692.

Amrani A. (2014) Organosulfur compounds: molecular and isotopic evolution from biota to oil and gas. *Annu. Rev. Earth Planet. Sci.* **42**, 733–768.

Adkins J. F., McIntyre K. and Schrag D. P. (2002) The salinity, temperature, and delta O-18 of the glacial deep ocean. *Science (80-.)* **298**, 1769–1773.

Antler G., Turchyn A. V., Rennie V., Herut B. and Sivan O. (2013) Coupled sulfur and oxygen isotope insight into bacterial sulfate reduction in the natural environment. *Geochim. Cosmochim. Acta* **118**, 98–117.

Balci N., Shanks W. C., Mayer B. and Mandernack K. W. (2007) Oxygen and sulfur isotope systematics of sulfate produced by bacterial and abiotic oxidation of pyrite. *Geochim. Cosmochim. Acta* **71**, 3796–3811.

Balci N., Mayer B., Shanks W. C. and Mandernack K. W. (2012) Oxygen and sulfur isotope systematics of sulfate produced during abiotic and bacterial oxidation of sphalerite and elemental sulfur. *Geochim. Cosmochim. Acta* **77**, 335–351.

Berner R. A. (1982) Burial of organic carbon and pyrite sulfur in the modern ocean; its geochemical and environmental significance. *Am. J. Sci.* **282**, 451–473.

Bishop J. K. B. (1988) The barite-opal-organic carbon association in oceanic particulate matter. *Nature* **332**, 341–343.

Bjerrum C. J., Bendtsen J. and Legarth J. J. F. (2006) Modeling organic carbon burial during sea level rise with reference to the Cretaceous. *Geochem. Geophys. Geosyst.* **7**.

Blake R. E., Surkov A. V., Böttcher M. E., Ferdelman T. G. and Jorgensen B. B. (2006) Oxygen isotope composition of dissolved sulfate in deep-sea sediments: Eastern equatorial Pacific Ocean. *Proc. Ocean Drill. Program Sci. Results* **201**, 1–23.

Böhlke J. K., Mroczkowski S. J. and Coplen T. B. (2003) Oxygen isotopes in nitrate: new reference materials for ^{18}O:^{17}O:^{16}O measurements and observations on nitrate-water equilibration. *Rapid Commun. Mass Spectrom.* **17**, 1835–1846. Available at: <http://www.ncbi.nlm.nih.gov/pubmed/12876683> (Accessed December 23, 2014).

Böttcher M. E., Brumsack H.-J. and De Lange G. J. (1998) Sulfate reduction and related stable isotope (^{34}S, ^{18}O) variations in interstitial waters from the Eastern Mediterranean. *Proc. Ocean Drill. Program Sci. Results* **160**, 365–373.

Böttcher M. E., Bernasconi S. M. and Brumsack H.-J. (1999) Carbon, sulfur, and oxygen isotope geochemistry of interstitial waters from the western mediterranean. In *Proceedings of the Ocean Drilling Program, Scientific Results*. pp. 413–421.

Böttcher M. E., Thamdrup B. and Vennemann T. W. (2001a) Anaerobic sulfide oxidation and stable isotope fractionation associated with bacterial sulfur disproportionation in the presence of MnO_2. *Geochim. Cosmochim. Acta* **65**, 1573–1581.

Böttcher M. E., Thamdrup B. and Vennemann T. W. (2001b) Oxygen and sulfur isotope fractionation during anaerobic bacterial disproportionation of elemental sulfur. *Geochim. Cosmochim. Acta* **65**, 1601–1609.

Böttcher M. E., Thamdrup B., Gehre M. and Theune A. (2005) S-34/S-32 and O-18/O-16 fractionation during sulfur disproportionation by *Desulfobulbus propionicus*. *Geomicrobiol. J.* **22**, 219–226.

Bottrell S. H. and Newton R. J. (2006) Reconstruction of changes in global sulfur cycling from marine sulfate isotopes. *Earth Sci. Rev.* **75**, 59–83.

Bowles M. W., Mogollón J. M., Kasten S., Zabel M. and Hinrichs K.-U. (2014) Global rates of marine sulfate reduction and implications for sub-sea-floor metabolic activities. *Science* **344**, 889–891.

Brand W. A., Coplen T. B., Aerts-Bijma A. T., Böhlke J. K., Gehre M., Geilmann H., Gröning M., Jansen H. G., Meijer H. A. J., Mroczkowski S. J., Qi H., Soergel K., Stuart-Williams H., Weise S. M. and Werner R. A. (2009) Comprehensive inter-laboratory calibration of reference materials for $\delta^{18}O$ versus VSMOW using various on-line high-temperature conversion techniques. *Rapid Commun. Mass Spectrom.* **23**, 999–1019.

Breit G. N., Simmons E. C. and Goldhaber M. B. (1985) Dissolution of barite for the analysis of strontium isotopes and other chemical and isotopic variations using aqueous sodium carbonate. *Chem. Geol.* **52**, 333–336.

Brunner B. and Bernasconi S. M. (2005) A revised isotope fractionation model for dissimilatory sulfate reduction in sulfate reducing bacteria. *Geochim. Cosmochim. Acta* **69**, 4759–4771.

Brunner B., Einsiedl F., Arnold G. L., Müller I., Templer S. and Bernasconi S. M. (2012) The reversibility of dissimilatory sulphate reduction and the cell-internal multi-step reduction of sulphite to sulphide: insights from the oxygen isotope composition of sulphate. *Isot. Environ. Health Stud.* **48**, 33–54.

Burdige D. J. and Nealson K. H. (1986) Chemical and microbiological studies of sulfide-mediated manganese reduction. *Geomicrobiol. J.* **4**(4), 361–387.

Canfield D. E. (1989) Reactive iron in marine sediments. *Geochim. Cosmochim. Acta* **53**, 619–632.

Canfield D. E. (2001) Biogeochemistry of Sulfur Isotopes. *Rev. Mineral. Geochem.* **43**, 607–636.

Canfield D. E. and Thamdrup B. (1994) The production of ^{34}S-depleted sulfide during bacterial disproportionation of elemental sulfur. *Science* **266**, 1973–1975.

Canfield D. E. and Thamdrup B. (1996) Fate of elemental sulfur in an intertidal sediment. *FEMS Microbiol. Ecol.* **19**, 95–103.

Canfield D. E., Jorgensen B. B., Fossing H., Glud R., Gundersen J., Ramsing N. B., Thamdrup B., Hansen J. W., Nielsen L. P. and Hall P. O. (1993) Pathways of organic carbon oxidation in three continental margin sediments. *Mar. Geol.* **113**, 27–40.

Chiba H. and Sakai H. (1985) Oxygen isotope exchange rate between dissolved sulfate and water at hydrothermal temperatures. *Geochim. Cosmochim. Acta* **49**, 993–1000.

Chow T. J. and Goldberg E. D. (1960) On the marine geochemistry of barium. *Geochim. Cosmochim. Acta* **20**, 192–198.

Cleveland W. S. (1979) Robust locally weighted regression and smoothing scatterplots. *J. Am. Stat. Assoc.* **74**, 829–836. Available at: <http://www.jstor.org/stable/2286407>.

Coplen T. B., Hopple J. A., Böhlke J. K., Peiser H. S., Rieder S. E., Krouse H. R., Rosman K. J. R., Ding T., Vocke R. D. J., Révész K. M., Lamberty A., Taylor P. and Bièvre P. De (2001) *Compilation of minimum and maximum isotope ratios of selected elements in naturally occurring terrestrial materials and reagents*. Available at: <http://pubs.usgs.gov/wri/wri014222/>.

DeBond N., Oakes R. L., Paytan A. and Wortmann U. G. (2012) Early Aptian carbon and sulphur isotope signatures at ODP Site 765. *Isot. Environ. Health Stud.* **48**, 180–194.

Dehairs F., Chesselet R. and Jedwab J. (1980) Discrete suspended particles of barite and the barium cycle in the open ocean. *Earth Planet. Sci. Lett.* **49**, 528–550.

D'Hondt S., Rutherford S. and Spivack A. J. (2002) Metabolic activity of subsurface life in deep-sea sediments. *Science* **295**, 2067–2070.

Eckert T., Brunner B., Edwards E. A. and Wortmann U. G. (2011) Microbially mediated re-oxidation of sulfide during dissimilatory sulfate reduction by *Desulfobacter latus*. *Geochim. Cosmochim. Acta* **75**, 3469–3485.

Farquhar J., Canfield D. E., Masterson A., Bao H. and Johnston D. (2008) Sulfur and oxygen isotope study of sulfate reduction in experiments with natural populations from Fellestrand, Denmark. *Geochim. Cosmochim. Acta* **72**, 2805–2821.

Ferdelman T. G., Lee C., Pantoja S., Harder J., Bebout B. M. and Fossing H. (1997) Sulfate reduction and methanogenesis in a Thioploca-dominated sediment off the coast of Chile. *Geochim. Cosmochim. Acta* **61**, 3065–3079.

Fritz P., Basharmal G. M., Drimmie R. J., Ibsen J. and Qureshi R. M. (1989) Oxygen isotope exchange between sulphate and water during bacterial reduction of sulphate. *Chem. Geol.* **79**, 99–105. Available at: <http://www.sciencedirect.com/science/article/pii/0168962289900122> (Accessed December 23, 2014).

Froelich P. N., Klinkhammer G. P., Bender M. L., Luedtke N. A., Heath G. R., Cullen D., Dauphin P., Hammond D., Hartman B. and Maynard V. (1979) Early oxidation of organic matter in pelagic sediments of the eastern equatorial Atlantic: suboxic diagenesis. *Geochim. Cosmochim. Acta* **43**, 1075–1090.

Ganeshram R. S., François R., Commeau J. and Brown-Leger S. L. (2003) An experimental investigation of barite formation in seawater. *Geochim. Cosmochim. Acta* **67**, 2599–2605.

Griffith E. M. and Paytan A. (2012) Barite in the ocean – occurrence, geochemistry and palaeoceanographic applications. *Sedimentology* **59**, 1817–1835.

Hansen K. W. and Wallmann K. (2003) Cretaceous and cenozoic evolution of seawater composition, atmospheric O_2 and CO_2: a model perspective. *Am. J. Sci.* **303**, 94–148.

Hay W. W. and Southam J. R. (1977) Modulation of marine sedimentation by the continental shelves. In *The Fate of Fossil Fuel CO2 in the Oceans* (eds. N. R. Andersen and A. Malahoff). Plenum Press, pp. 569–604.

Hedges J. I. and Keil R. G. (1995) Sedimentary organic matter preservation: an assessment and speculative synthesis. *Mar. Chem.* **49**, 137–139.

Hoefs J. (2009) *Stable Isotope Geochemistry*. Springer Science & Business Media.

Holser W. T., Kaplan I. R., Sakai H. and Zak I. (1979) Isotope geochemistry of oxygen in the sedimentary sulfate cycle. *Chem. Geol.* **25**, 1–17.

Jacquet S. H. M., Henjes J., Dehairs F., Worobiec A., Savoye N. and Cardinal D. (2007) Particulate Ba-barite and acantharians in the Southern Ocean during the European iron fertilization experiment (EIFEX). *J. Geophys. Res.* **112**, G04006.

Johnston D. T., Gill B. C., Masterson A., Beirne E., Casciotti K. L., Knapp A. N. and Berelson W. (2014) Placing an upper limit on cryptic marine sulphur cycling. *Nature* **513**, 530–533.

Jørgensen B. B. (1982) Mineralization of organic matter in the sea bed – the role of sulphate reduction. *Nature* **296**, 643–645. http://dx.doi.org/10.1038/296643a0.

Jørgensen B. B. (1990) A thiosulfate shunt in the sulfur cycle of marine sediments. *Science* **249**, 152–154.

Jørgensen B. B. and Kasten S. (2006) Sulfur cycling and methane oxidation. In *Marine Geochemistry*, pp. 271–309.

Kohl I. and Bao H. (2011) Triple-oxygen-isotope determination of molecular oxygen incorporation in sulfate produced during abiotic pyrite oxidation (pH = 2–11). *Geochim. Cosmochim. Acta* **75**, 1785–1798.

Kump L. R. (1989) Alternative modeling approaches to the geochemical cycles of carbon, sulfur, and strontium isotopes. *Am. J. Sci.* **289**, 390–410.

Lichtschlag A., Felden J., Brüchert V., Boetius A. and de Beer D. (2010) Geochemical processes and chemosynthetic primary production in different thiotrophic mats of the Håkon Mosby Mud Volcano (Barents Sea). *Limnol. Oceanogr.* **55**, 931–949.

Lisiecki L. E. and Raymo M. E. (2005) A Plio-Pleistocene stack of 57 globally distributed benthic [delta]^{18}O records. *Paleoceanography* **20**, PA1003.

Llyod R. M. (1967) Oxygen-18 composition of oceanic sulfate. *Science* **156**, 1228–1231.

Lloyd R. M. (1968) Oxygen isotope behavior in the sulfate-water system. *J. Geophys. Res.* **73**, 6099.

Markovic S., Paytan A. and Wortmann U. G. (2015) Pleistocene sediment offloading and the global sulfur cycle. *Biogeosciences* **12**, 3043–3060. http://dx.doi.org/10.5194/bg-12-3043-2015.

Miller K., Mountain G., Wright J. and Browning J. (2011) A 180-million-year record of sea level and ice volume variations from continental margin and deep-sea isotopic records. *Oceanography* **24**, 40–53.

Monnin C., Jeandel C., Cattaldo T. and Dehairs F. (1999) The marine barite saturation state of the world's oceans. *Mar. Chem.* **65**, 253–261.

Oguz T., Murray J. W. and Callahan A. E. (2001) Modeling redox cycling across the suboxic–anoxic interface zone in the Black Sea. *Deep Sea Res. Part I* **48**, 761–787.

Paytan A. and Griffith E. M. (2007) Marine barite: Recorder of variations in ocean export productivity. *Deep Res. Part II* **54**, 687–705.

Paytan A., Kastner M. and Chavez F. P. (1996) Glacial to interglacial fluctuations in productivity in the equatorial pacific as indicated by marine barite. *Science (80-.)* **274**, 1355–1357.

Paytan A., Mearon S., Cobb K. and Kastner M. (2002) Origin of marine barite deposits: Sr and S isotope characterization. *Geology* **30**, 747–750.

R Development Core Team (2013) *R: A Language and Environment for Statistical Computing*. R Foundation for Statistical Computing, Vienna, Austria, URL: <http://www.R-project.org/>.

Rees C. E. (1973) A steady-state model for sulphur isotope fractionation in bacterial reduction processes. *Geochim. Cosmochim. Acta* **37**, 1141–1162.

Richter F. M. and Turekian K. K. (1993) Simple models for the geochemical response of the ocean to climatic and tectonic forcing. *Earth Planet. Sci. Lett.* **119**, 121–131.

Rushdi A. I., McManus J. and Collier R. W. (2000) Marine barite and celestite saturation in seawater. *Mar. Chem.* **69**, 19–31.

Schrag D. P., Hampt G. and Murray D. W. (1996) Pore fluid constraints on the temperature and oxygen isotopic composition of the glacial ocean. *Science (80-.)* **272**, 1930–1932.

Schrag D. P., Adkins J. F., McIntyre K., Alexander J. L., Hodell D. A., Charles C. D. and McManus J. F. (2002) The oxygen isotopic composition of seawater during the last glacial maximum. *Quat. Sci. Rev.* **21**, 331–342.

Shackleton N. (1967) Oxygen isotope analyses and pleistocene temperatures re-assessed. *Nature* **215**, 15–17.

Shackleton N. J. (1987) Oxygen isotopes, ice volume and sea level. *Quat. Sci. Rev.* **6**, 183–190.

Shackleton N. J., Crowhurst S., Hagelberg T., Pisias N. G. and Schneider D. A. (1995) A new late Neogene time scale: Application to Leg 138 sites. In *Proceedings of the Ocean Drilling Program. Scientific Results Ocean Drilling Program*. pp. 73–101.

Shipboard Scientific Party (1992) Site 849. In *Proceedings of the Ocean Drilling Program, Initial Reports, 138, College Station, TX* (*Ocean Drilling Program*), pp. 735–807.

Schulz H. D., Dahmke A., Schinzel U., Wallmann K. and Zabel M. (1994) Early diagenetic processes, fluxes, and reaction rates in sediments of the South Atlantic. *Geochim. Cosmochim. Acta* **58**, 2041–2060.

Sørensen J., Jørgensen B. B. and Revsbech N. P. (1979) A comparison of oxygen, nitrate, and sulfate respiration in coastal marine sediments. *Microb. Ecol.* **5**, 105–115.

Von Allmen K., Böttcher M. E., Samankassou E. and Nägler T. F. (2010) Barium isotope fractionation in the global barium cycle: first evidence from barium minerals and precipitation experiments. *Chem. Geol.* **277**, 70–77.

Van Stempvoort D. R. and Krouse H. R. (1994) Controls of $\delta^{18}O$ in sulfate review of experimental data and application to specific environments. In *Environmental Geochemistry of Sulfide Oxidation, ACS Symposium Series, vol. 550* (eds. C. N. Alpers and D. W. Blowes). American Chemical Society, Washington, D.C., pp. 446–480. Available at: <http://dx.doi.org/10.1021/bk-1994-0550.ch029> (Accessed December 23, 2014).

Taylor B. E., Wheeler M. C. and Nordstrom D. K. (1984) Isotope composition of sulphate in acid mine drainage as measure of bacterial oxidation. *Nature* **308**, 538–541.

Thamdrup B., Finster K., Hansen J. W. and Bak F. (1993) Bacterial disproportionation of elemental sulfur coupled to chemical reduction of iron or manganese. *Appl. Environ. Microbiol.* **59**, 101–108.

Thamdrup B., Fossing H. and Jørgensen B. B. (1994) Manganese, iron and sulfur cycling in a coastal marine sediment, Aarhus Bay, Denmark. *Geochim. Cosmochim. Acta* **58**, 5115–5129.

Thullner M., Dale A. W. and Regnier P. (2009) Global-scale quantification of mineralization pathways in marine sediments: a reaction-transport modeling approach. *Geochem. Geophys. Geosyst* **10**.

Torres M. E., Brumsack H. J., Bohrmann G. and Emeis K. C. (1996) Barite fronts in continental margin sediments: a new look at barium remobilization in the zone of sulfate reduction and formation of heavy barites in diagenetic fronts. *Chem. Geol.* **127**, 125–139.

Turchyn A. V. and Schrag D. P. (2004) Oxygen isotope constraints on the sulfur cycle over the past 10 million years. *Science* **303**, 2004–2007.

Turchyn A. V. and Schrag D. P. (2006) Cenozoic evolution of the sulfur cycle: insight from oxygen isotopes in marine sulfate. *Earth Planet. Sci. Lett.* **241**, 763–779.

Turchyn A. V., Sivan O. and Schrag D. P. (2006) Oxygen isotopic composition of sulfate in deep sea pore fluid: evidence for rapid sulfur cycling. *Geobiology* **4**, 191–201.

Turchyn A. V., Brüchert V., Lyons T. W., Engel G. S., Balci N., Schrag D. P. and Brunner B. (2010) Kinetic oxygen isotope effects during dissimilatory sulfate reduction: a combined theoretical and experimental approach. *Geochim. Cosmochim. Acta* **74**, 2011–2024.

Walton G. and Walden G. H. (1946a) The Contamination of precipitated barium sulfate by univalent cations 1. *J. Am. Chem. Soc.* **68**, 1742–1750. http://dx.doi.org/10.1021/ja01213a018.

Walton G. and Walden G. H. (1946b) The nature of the variable hydration of precipitated barium sulfate 1. *J. Am. Chem. Soc.* **68**, 1750–1753. http://dx.doi.org/10.1021/ja01213a019.

Wankel S. D., Bradley A. S., Eldridge D. L. and Johnston D. T. (2014) Determination and application of the equilibrium oxygen isotope effect between water and sulfite. *Geochim. Cosmochim. Acta* **125**, 694–711.

Wollast R. (1991) The coastal organic carbon cycle: fluxes, sources and sinks. In *Ocean Margin Processes in Global Change*, pp. 365–382.

Wortmann U. G., Chernyavsky B., Bernasconi S. M., Brunner B., Böttcher M. E. and Swart P. K. (2007) Oxygen isotope biogeochemistry of pore water sulfate in the deep biosphere: dominance of isotope exchange reactions with ambient water during microbial sulfate reduction (ODP Site 1130). *Geochim. Cosmochim. Acta* **71**, 4221–4232.

Zopfi J., Böttcher M. E. and Jørgensen B. B. (2008) Biogeochemistry of sulfur and iron in Thioploca-colonized surface sediments in the upwelling area off Central Chile. *Geochim. Cosmochim. Acta* **72**, 827–843.

Associate editor: James Farquhar